Евразиатский энтомол. журнал 21(Приложение 1): 23–41
doi 10.15298/euroasentj.21.Spl.1.04

New insights on *Diamesa* Meigen (Diptera, Chironomidae, Diamesinae) in the Tibetan Plateau of China

Новые данные о *Diamesa* Meigen (Diptera, Chironomidae, Diamesinae) с Тибетского нагорья в Китае

Wu Han*, Lili Wei, Zhenyu Ni*, Hongqu Tang**, *****
Ву Хань*, Лили Ви, Цхенью Ни*, Хунк Тан**, *****

* State Key Laboratory of Lake Science and Environment, Nanjing Institute of Geography and Limnology, Chinese Academy of Science, Nanjing 210008 China.

* Государственная головная лаборатория наук об озерах и окружающей среде, Нанкинский институт географии и лимнологии Китайской академии наук, Нанкин 210008 Китай.

** Life Science and Technology College, Jinan University, Guangzhou 510632 China.

** Колледж биологических наук и технологий Цзинаньского университета, Гуанчжоу 510632 Китай.

***Correspondence author: townningt@gmail.com.

Key words: *Diamesa*, Tibetan Plateau, new species, pupa, larva, DNA barcoding, distribution.

Ключевые слова: *Diamesa,* Тибетское нагорье, новые виды, куколки, личинки, ДНК-баркодинг, распространение.

Abstract. *Diamesa* Meigen (Diptera: Chironomidae) is an extremely cold-adapted common representative of the subfamily Diamesinae, yet famous also in the Tibetan Plateau, but already threatened due to ongoing reduction and loss of glaciers. To provide baseline information about species richness, distribution pattern and ecological preferences, larva, pupa and adult materials of *Diamesa* collected from 20 sampling sites in the Tibet Plateau were analyzed based morphology and DNA barcoding technique. In total, 14 *Diamesa* species (including molecular operational taxonomic units) were delimitated, of which 2 are known species, 2 are new to science, and other 10 are putative molecular species (OTUs). Among them, *D. pseudosteinboecki* **sp.n.** and *D. kandzensis* **sp.n.** are here established as new species based on all stages. *D. kaszabi* Serra-Tosio is formally recorded in Tibet, China for the first time and *D. qiangi* Wang et Makarchenko is reconfirmed in the Tibet region. For the first time the immature stages of above two species are described through DNA barcoding linkage and pharate material. Due to the absence of associated adult males, the taxonomic status of the 10 putative molecular taxa could not be determined here formally but simple comparative diagnosis are given on available larval or pupal stages. The distribution pattern and ecological data of these species/OTUs are provided here as well. Our study suggests that biodiversity over Tibetan Plateau have been poorly explored, massive fundamental works are urgently needed for effective ecosystem protection.

Резюме. *Diamesa* Meigen (Diptera: Chironomidae) — чрезвычайно адаптированный к холоду обычный представитель подсемейства Diamesinae, известный также с Тибетского нагорья, но уже находящийся под угрозой из-за продолжающегося сокращения и потери ледников. Чтобы получить исходную информацию о видовом богатстве, характере распространения и экологических предпочтениях, личинки, куколки и имаго *Diamesa,* собранные в 20 локациях на Тибетском плато, были проанализированы на морфологическом и молекулярно-генетическом уровнях. Всего выделено 14 видов *Diamesa* (включая молекулярные операционные таксономические единицы), из них 2 известных вида, 2 новых для науки и 10 предполагаемых молекулярных видов (OTU). Среди них *D. pseudosteinboecki* **sp.n.** и *D. kandzensis* **sp.n.** описаны как новые виды по трем стадиям развития. *D. kaszabi* Serra-Tosio впервые зарегистрирован для Тибета и Китая, а *D. qiangi* Wang et Makarchenko повторно подтвержден в Тибетском регионе. Впервые преимагинальные стадии двух вышеупомянутых видов описаны с помощью ДНК-анализа и материала выведения. Из-за отсутствия ассоциированных взрослых самцов таксономический статус 10 предполагаемых молекулярных таксонов не может быть определен формально, но дается простой сравнительный диагноз и иллюстрации для их личинок или куколок. Также представлены типы распространения и экологические данные для этих видов/OTU. Наше исследование показало, что биоразнообразие над Тибетским нагорьем изучено слабо, для эффективной защиты экосистем срочно необходимы масштабные фундаментальные работы.

Introduction

Diamesa Meigen, also known as snow midges, is a species-diverse genus of the subfamily Diamesinae, comprising of ca. 120 valid species worldwide so far [Ashe, O'Connor, 2009; Makarchenko, 2022, pers. comm.]. Many species of this genus show tolerate cold and harsh environment and often act as pioneer colonizers in deglaciated terrains [Milner et al., 2008]. Larvae of *Diamesa* are dominant in alpine springs and kryon zone of glacier-fed streams [Flory, Milner, 2000; Anderson et al., 2013]. However, the cold stenothermal trait of some *Diamesa* species may predispose them to increased risk of extinction as the warming climate rap-

idly ameliorates their harsh environment [Lencioni, 2018; Lencioni et al., 2021a].

As the world's third-largest repository of ice, many glaciers distributed on the Tibetan Plateau depend on the extreme altitude and great development of paleoplanation surface [Sun et al., 2019a]. Theoretically, the extensive development of glaciers provides suitable habitats for *Diamesa*. Totally, thirty species have been recorded on the Tibet Plateau and its surrounding regions, including Nepal, Afghanistan, Kirgizstan, Tajikistan, Uzbekistan, and also its northern extension, Tien Shan Mt (Table 1). Though four Indian species, *D. bryophila* (Singh, 1958), *D. dashauhari* Singh et Maheshwari, 1989, *D. khoksarensis* (Kaul, 1970) and *D. virendri* (Singh, 1958), are counted here as well, these records are unconfirmed by other studies. Currently, the Tibetan Plateau is undergoing the warmest period during the past 2,000 years, with air temperatures rising twice the global average rate [Chen et al., 2020; Zhang et al., 2020]. The Tibetan Plateau glaciers show a significant reduction trend over the past four decades, with accelerating recent melting as the result of rising temperatures [Ye et al., 2006; Wang et al., 2013; Sun et al., 2019a]. Since their preference in living glacier-fed streams, glacial retreat on the Tibetan Plateau elevates extinction risk of some oligo-stenothermal *Diamesa* species [Hamerlik, Jacobsen, 2012]. Thus, it is urgent to understand the species richness, distribution pattern and ecology characteristics of *Diamesa* for an effective conservation of local biodiversity. However, taxonomic studies on Diamesa in the Tibetan Plateau are inadequate excepting sporadic records during recent decades [Willassen, 2005; Sun et al., 2019b; Lin et al., 2021].

Morphological taxonomy of Chironomidae is usually tedious, and sometimes ineffective for larvae since few discriminating features are visible [Curry et al., 2018]. For *Diamesa*, morphological identification of larvae is very challenging because some valuable characters such as mental and mandibular teeth are often worn excessively in field-collected specimens [Rossaro, Lencioni, 2015]. With the development of sequencing tech-

Table 1. The known species of *Diamesa* Meigen occurred in the Tibet Plateau and its surroundings
Таблица 1. Известные виды *Diamesa* Meigen, обнаруженные на Тибетском плато и в его окрестностях

Species name	Zoogeographic region	Distribution
Diamesa aberrata Lundbeck, 1898	HA, OR	Canada; USA; Russia; India (Jammu-Kashmir)
Diamesa aculeata Willassen, 2005	PA	China (Tibet)
Diamesa akhrorovi Makarchenko et Semenchenko, 2018	PA	Tajikistan (Pamir Mountains)
Diamesa alibaevae Makarchenko et Semenchenko, 2018	PA	Kirgizstan (Tien Shan)
Diamesa amanoi Makarchenko et Kobayashi, 1997	OR, PA	Nepal; China (Xinjiang: Tien Shan)
Diamesa barraudi Pagast, 1947	OR	India (Himachal Pradesh); Nepal
Diamesa bertrami Edwards, 1935	PA	China (Xinjiang)
Diamesa filicauda Tokuanga, 1966	PA	Afghanistan; Uzbekistan; China (Qinghai)
Diamesa insidiosa Serra-Tosio, 1983	OR	Nepal
Diamesa kasaulica Pagast, 1947	OR	India (Jammu-Kashmir); Nepal
Diamesa khumbugelida Sæther et Willassen, 1987	OR, PA	Nepal; Tajikistan; Russia (Khakassia; Baikal Lake basin)
Diamesa kohshimai Sæther et Willassen, 1987	OR	Nepal
Diamesa loeffleri Reiss, 1968	PA, OR	Afghanistan; Nepal; China (Qinghai)
Diamesa maisaraensis Makarchenko et Semenchenko, 2022	PA	Tajikistan (Pamir Mountains)
Diamesa marinskiyi Makarchenko et Semenchenko, 2022	PA	China (Xinjiang, Tien Shan)
Diamesa planistyla Reiss, 1968	OR; PA	Nepal; Kirgizstan (Tien Shan); China (Xinjiang); Tajikistan
Diamesa praecipua Sæther et Willassen, 1987	OR	Nepal; India (Himalayas)
Diamesa qiangi Wang et Makarchenko, 2019	PA	China (Tibet)
Diamesa solhoyi Willassen, 2005	PA	China (Tibet)
Diamesa steinboecki Goetghebuer, 1933	PA	Europe Alps; Tajikistan (Pamir)
Diamesa stenonyx Serra-Tosio, 1983	OR	Nepal
Diamesa tenuescens Serra-Tosio, 1983	OR	India (Jammu and Kashmir)
Diamesa yalavia Sæther et Willassen, 1987	OR	Nepal
Diamesa kaszabi Serra-Tosio, 1983	PA	Tajikistan; Mongolia; China (Qinghai)
Diamesa zhiltzovae Makarchenko, 1989	PA	Tajikistan
Diamesa tonsa (Haliday, 1856)	PA	Afghanistan; Europe; Russia
?Diamesa bryophila (Singh, 1958)	OR	India (Himachal Pradesh)
?Diamesa dashauhari Singh et Maheshwari, 1989	PR	India (Himachal Pradesh)
?Diamesa khoksarensis (Kaul, 1970)	OR	India (Himachal Pradesh)
?Diamesa virendri (Singh, 1958)	OR	India (Himachal Pradesh)

niques, the plight of traditional taxonomy has been relieved by the adaption of DNA barcoding (Hebert, Gregory, 2005). So far, barcoding has been widely utilized in Chironomidae studies to delimit species, associate different life stages and discover cryptic species [Ekrem et al., 2010; Stur et al., 2011; Lin et al., 2018].

The Second Expedition Program of Tibetan Plateau (2019–2021) offers us a great opportunity to investigate the biodiversity of the family Chironomidae on the highest plateau. In this study, we provide a preliminarily report on the richness and distribution of *Diamesa* from the Plateau based on both morphological taxonomy and DNA barcoding techniques. Besides, photos, illustration and, geographic and ecological data of determined species are provided as references for further studies.

Material and method

Specimens were collected from over 100 sites, including ponds, lakes, rivers and streams over Tibetan Plateau in the summer of 2018, 2020 and 2021 (Fig. 1, Table 2). Different sampling strategies were adopted to lotic and lentic ecosystems respectively. For lakes, pupal and larval exuviae and drowned adults were

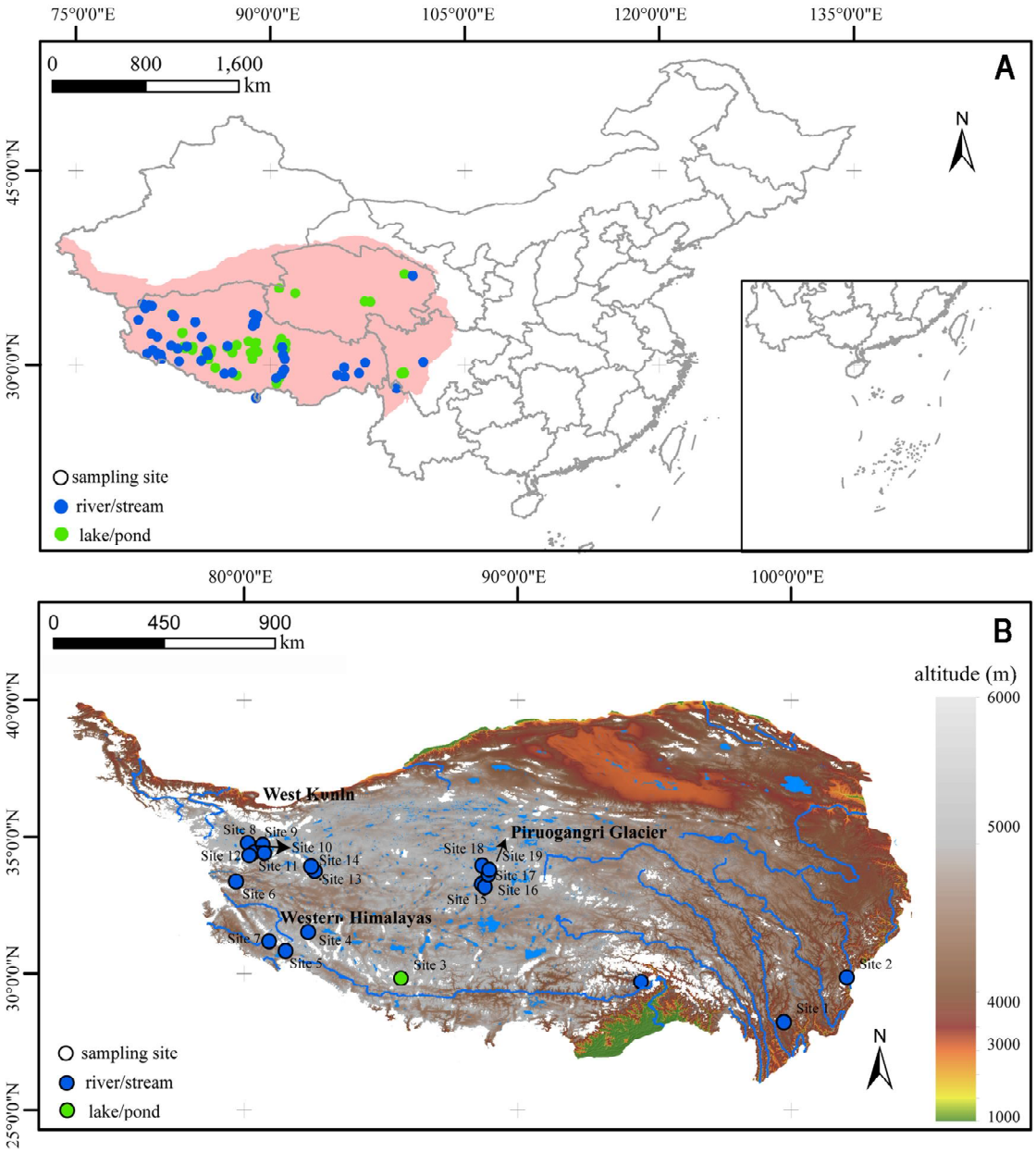

Fig. 1. Distribution of sampling sites. Up, all surveyed sites during the field trip; down, the sample sites with *Diamesa*, white patches indicating the distribution of glaciers on the Tibetan Plateau (GLIMS, 2005).

Рис. 1. Распределение мест отбора проб. Вверху — все обследованные участки во время полевых работ; внизу — пробные участки с *Diamesa*, белые пятна указывают на распространение ледников на Тибетском плато (GLIMS, 2005 г.).

collected with a drift net (mesh size 250 μm). Living larvae in lake sediment were collected using a Peterson grab and a benthic trawl. For rivers and streams, immature materials were sampled with dip nets intersecting running waters (mesh size 250μm). Adults were caught using sweep nets along the shores of lakes and rivers. Immature materials were washed and filtered in situ, then stored in plastic sealed bags with 95 % ethanol while adults were preserved in 5ml centrifuge tubes with 85 % ethanol. Physicochemical factors were measured in situ using YSI EXO2 Multiparameter Sonde (YSI Inc./Xylem Inc., Yellow Springs, OH, USA). The distribution of glaciers was obtained from Randolph Glacier Inventory, which was released by Global Land Ice Measurements from Space (GLIMS, http://www.glims.org/RGI/) in 2015 [NSIDC, 2019]. The boundary of Tibetan Plateau in China was downloaded from the National Tibetan Plateau Data Center [Zhang et al., 2019].

Specimens were dissected and mounted on the slides with Euparal. General morphological terminology and abbreviations followed Sæther [1980] except for male genitalia, for which suggestions from Montagna et al. [2016] were adopted here. Measurements are given as ranges and followed by average value. Some additional new abbreviations are listed as follows. A1R: basal antenna ratio, basal segment divided by the width through the ring organ; AAII: anterior anepisternum II of adult thorax; HR: horn ratio, total length of thoracic horn divided by the basal width; ROR: ring organ ratio, location of ring organ from the base divided by the total basal segment; SPR: the distance of distal setal pit from the base divided by the basal antennal segment length; PPr: posterior parapods ratio, the total length of posterior parapods divided by the sub-basal width through the constriction. All type specimens have been deposited in the College of Life Science and Technology, Jinan University.

Bodies of larvae and thorax of pupae and adults were picked out for molecular study. DNA was extracted using the MAGEN® (Beijing, China) Tissue DNA kit, following the standard protocol provided by the manufacturer. Universal primers LCO1490 (ggt caa caa atc ata aag ata ttg g) and HCO2198 (taa act tca ggg tga cca aaa aat ca) [Folmer et al., 1994] were adopted to amplify the standard barcode region of mitochondrial cytochrome c oxidase subunit I (COI). Mitochondrial cytochrome c oxidase subunit II (COII) fragments were amplified with the standard primers TL2-J- 3034 (aat atg gca gat tag tgc a) and TK-N-3785 *alias* B-tLYS (gtt taa gag acc agt act tg) [Simon et al., 1994]. Programs for amplification of gene fragments followed previous studies [Han, Tang 2019; Han et al., 2020]. PCR products were electrophoresed in 1.0 % agarose gel and shipped to Sangon Biotech Company, Guangzhou for purification and bidirectional sequencing.

Table 2. The location and habitat types of the sampling sites
Таблица 2. Расположение мест отбора проб и типы местообитаний

Site	Province	City/ Prefecture	Exact Region	Habit	Lat.,°N	Lon.,°E	Elev.,m	Collector	Collect Date
Site 01	Yunan	Shangri-La	Geza Township, unnamed stream	Stream	28.21	99.74	2958	X. Wen	19.vi.2018
Site 02	Sichuan	Garze	Luding County, Hongshitan of Hailuogou Scenic Spot	Stream	29.84	102.04	3051	X. Wen	27.vi.2020
Site 03	Tibet	Shikatse	Ngamring County, Takkyel Tso (Daggyai Co)	Lake	29.81	85.75	5145	W. Han	20.viii.2020
Site 04	Tibet	Ngari	Geji County, Yare Township, Wamo Zangbo	River	31.50	82.35	4816	W. Han	1.ix.2020
Site 05	Tibet	Ngari	Purang County, unnamed stream	Stream	30.82	81.54	4618	Z.Y. Ni	31.vii.2021
Site 06	Tibet	Ngari	Rutog County, Marka Zangbo	River	33.36	79.71	4282	W. Han	1.viiI.2021
Site 07	Tibet	Ngari	Gar County,Yarqu River	River	31.17	80.93	4712	Z.Y. Ni.	1.viii.2021
Site 08	Tibet	Ngari	Rutog County, Spring River	River	34.76	80.14	5126	W. Han	13.viii.2021
Site 09	Tibet	Ngari	Rutog County, Songxi village, unnamed stream	Stream	34.43	80.38	5202	W. Han	8.viii.2021
Site 10	Tibet	Ngari	Rutog County, unnamed stream	Stream	34.62	80.65	5163	W. Han	9.viii.2021
Site 11	Tibet	Ngari	Rutog County, unnamed stream	Stream	34.40	80.36	5368	W. Han	11.viii.2021
Site 12	Tibet	Ngari	Rutog County, Nanzhi River	Stream	34.57	80.86	5368	W. Han	13.viii.2021
Site 13	Tibet	Ngari	Geji County, unnamed stream	Stream	33.75	82.59	5139	W. Han	19.viii.2021
Site 14	Tibet	Ngari	Geji County, unnamed stream near Lalu Co	Stream	33.92	82.46	4939	W. Han	19.viii.2021
Site 15	Tibet	Ngari	Rutog County, unnamed stream	River	33.26	88.71	5247	W. Han.	26.viii.2021
Site 16	Tibet	Nagqu	Shuanghu County, unnamed stream	Stream	33.17	88.82	4910	W. Han.	27.viii.2021
Site 17	Tibet	Nagqu	Shuanghu County, Purog Kangri Glacier NNR	Spring	33.95	88.72	5080	W. Han.	29.viii.2021
Site 18	Tibet	Nagqu	Shuanghu County, Bingsha River	River	33.61	88.94	5134	W. Han.	29.viii.2021
Site 19	Tibet	Nagqu	Shuanghu County, unnamed stream	Stream	33.79	88.98	5330	W. Han.	29.viii.2021
Site 20	Tibet	Nyingchi	Dazi villaage	Stream	29.55	94.47	4282	J. Liu	8.vii.2014

Forward and reverse sequences were assembled automatically with SeqMan version 7.1.0 (in the LaserGene package, DNASTAR, Madison, USA). Contigs were aligned using Muscle algorithm [Edgar, 2004] on nucleotides and translated into amino acids to verify the presence of open reading frame in MEGA v 7.0 [Kumar et al., 2016]. The edited sequences were searched against the public *nt* database of the NCBI GeneBank (http://www.ncbi.nlm.nih.gov) for molecular identification and to exclude contamination and misidentification. These new-generated sequences were submitted to the BOLD system (http://www.boldsystems.org). The sequenced specimens with corresponding taxonomic information, collection sites and genetic markers can be seen online in the publicly accessible dataset «DS-TIBDIA. Barcodes of Tibetan *Diamesa*» [Ratnasingham, Hebert, 2007]. Some published DNA barcodes of *Diamesa* from previous studies [Montagna et al, 2016; Makarchenko et al., 2018, 2022; Lencioni et al., 2021b] were downloaded from the GeneBank. Besides, one COI sequence of *D. plumicornis* Tokunaga, 1936 (LC329089) from Japan and seven COI sequences of *D. qiangi* (MK185720–MK185726) were also mined from the public database. These downloaded barcodes were incorporated with our data to construct neighbor-joining (NJ) trees using the K2P model with 1000 bootstrap replicates and the «pairwise deletion» option for missing data in MEGA. One COI sequence of *Pseudodiamesa* Goetghebuer and three of *Pseudokiefferiella* (Edwards) were included in the dataset as outgroup following Lencioni et al. [2021b]. Pairwise distances were calculated using the Kimura 2 Parameter (K2P) substitution model in MEGA.

Automatic Barcode Gap Discovery (ABGD) [Puillandre et al., 2012] is an automatic procedure that partitions sequences into putative molecular species based on comparisons of pairwise distances. Our COI barcoding sequences were submitted to the online ABGD program (https://bioinfo.mnhn.fr/abi/public/abgd/abgdweb.html) for putative species delimitation. We applied the K2P model and relative barcode gap width of 1.0 to the analyses.

Results

Morphology taxonomy

Given the paucity of adult males and prevalence of immature larvae, most specimens from the Tibetan Plateau could not be morphologically identified deep into species level. Conservatively, we made preliminary division of pupae and larvae into coded morphotypes and based on complete stages determined two species as new to science.

Barcoding-based species delimitation

In total, 36 COI sequences (658 bp in length) and 17 COII sequences (378 and 680 bp) were obtained from 3 adult males, 2 adult females, 6 pupae and 25 larvae (Table 3). All mitochondrial sequences could be translated successfully into amino acids without indels and stop codons. The mean nucleotide base compositions were A 26.1 %, C 16.7 %, G 16.9 %, and T 40.3 % for COI genes while A 32.2 %, C 14.9 %, G 14.0 %, and T 38.9 % for COII genes.

The BLAST result suggested that all sequences belonged to the genus *Diamesa*. Four COI barcodes could be assigned reliably with a species name at an identity value threshold of 98 %. Other matches with low identity value (< 95 %) were excluded according to morphological taxonomy and geographic distribution information. The matched sequence (MK185726, identity value > 99.7 %) in the public database was labeled as *D. qiangi* Wang et Makarchenko, which was erected by Sun et al. (2019) based on adult males from the

Table 3. he distribution site, collected material and sequenced gene of the 14 species/taxa
Таблица 3. Место распространения, собранный материал и секвенированный ген 14 видов/таксонов

Species	Site Number	Life Stage	Molecular Data
D. kandzensis	S2	M, P, L	COI, COII
D. kaszabi	S3, S4, S8, S14, S17	M, F, P, L	COI
D. pseudosteinboecki	S8	M, P	COI, COII
D. qiangi	S5, S6, S7，S20	M, P, L	COI
D. sp.TP01	S13	L	COI
D. sp.TP02	S10	L	COI
D. sp.TP03	S15	L	COI
D. sp.TP04	S12, S15	L	COI, COII
D. sp.TP05	S2	P	COI, COII
D. sp.TP06	S1, S2	F, L	COI, COII
D. sp.TP07	S11	P	COI, COII
D. sp.TP08	S9, S13	L	COI, COII
D. sp.TP09	S16	L	COI, COII
D. sp.TP10	S9, S13, S18, S19	L	COI, COII

Designations: M — adult male, F — adult female, P — pupa, L — larva.
Условные обозначения: M — имаго самец; F — имаго самка; P — куколка; L — личинка

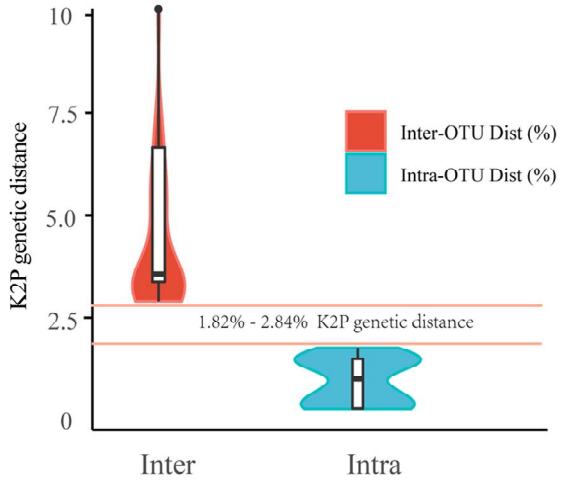

Fig. 2. Distribution of interspecific K2P distance and intraspecific distance among 14 putative molecular species.

Рис. 2. Распределение межвидовых расстояний (Кимура — 2 параметрическая модель) и внутривидовые расстояния среди 14 предполагаемых молекулярных видов.

southeastern Tibetan Plateau. Considering the matched sequences were submitted by the species erectors, the accuracy of the taxonomical annotation is reliable, thus three larvae and one pupae specimen were determined as *D. qiangi*. Searching against into Makarchenko's private COI database [2022, pers. comm.], revealed a morphological species including 7 larvae and 2 adult females as *Diamesa kaszabi* Serra-Tosio, 1983.

ABGD analysis produced 14 operational taxonomic units (OUTs) at a threshold of 0.77 % — 1.29 % intraspecific divergence for COI gene (Table 5). The species delimitation scheme produced by ABGD analysis generally was congruent with that of morphology taxonomy. However one morphological species comprised of 7 larvae was divided into two groups by ABGD. The mean interspecific K2P distance between the two groups (*D.* sp. TP08 and *D.* sp. TP10) was 3.6 % (Table 5). The maximum intraspecific K2P distance ranged from 0.32 % to 1.82 %, while minimum interspecific K2P distance ranged from 2.84 % to 10.08 % among these putative molecular species (Table 5). There is a small «barcoding gap» between the minimum interspecific and maximum intraspecific K2P distance (Fig. 2).

In total 243 COI sequences belonging to 30 *Diamesa* species were mined from the public database, including populations from Central Asia, European Alps, Japan, Russia and Tibetan Plateau. The 14 putative species were further confirmed on the N-J tree (Fig. 3), of which 12 species clustered with members of *aberrata* group. *D. pseudosteinboecki* sp.n. sank into *steinboecki* group while *D.* sp.TP05 fell outside any known groups. *D.* sp. TP06, which was morphologically similar with *D. plumicornis*, clustered with the Japanese *D. plumicornis*. However, the high genetic distance (> 5 %) between the Tibetan and Japanese populations suggested they were not conspecific. The N-J tree (Fig. 4) based on COII sequences shown a similar cluster pattern with that of COI sequences. However, our COII sequences did not match any species from South Tibeta described in Willassen (2005).

Distribution and Ecology

Over 50 lotic and 60 lentic water bodies have been surveyed during the past years (Fig.1A), but *Diamesa* was detected only in 20 sampling sites, mainly distributing in the northwestern Tibetan Plateau, the Western Himalayas and the Piruogangri Glacier (Fig. 1B). Though glaciers are well developed over the southeastern Tibetan Plateau, *Diamesa* was not detected here. The only lake where *Diamesa* were sampled was Daggyai Co (Table 2), located in the intermountain basin of Gangdise mountains, some with glaciers at the peaks. Thus, it seems the larvae in the lake were more likely transferred from surround alpine streams by glacier runoff. The most common species were *D. kaszabi* and *D.* sp. TP10 (Table 3). *D. qiangi* was recorded in southeastern Tibet (Linzi) previously, and its distribution is extended here to the western Himalayas. Other species could be found only in one or two sites. Most specimens were primarily attached to emergent/submerged gravels or pebbles with biofilm and physicochemical data of eleven sampling sites are provided in Table 4.

Table 4. Main physicochemical data of the 11 sampling sites. The ecological data of the other 8 sites were not measured

Таблица 4. Основные физико-химические данные 11 мест отбора проб. Экологические данные остальных 8 участков не измерялись

Site	pH	DO (mg/L)	WT (°C)	Cond. (μs/cm)	Salinity (ppt)
S03	9.41	6.20	11.95	NA	2.36
S08	7.79	5.49	3.10	296.90	0.19
S09	7.86	5.93	9.00	217.85	0.12
S10	7.57	6.61	4.40	109.00	0.07
S12	7.68	6.78	6.90	125.20	0.07
S13	7.84	5.99	9.60	217.50	0.12
S15	7.49	6.40	6.60	235.20	0.14
S16	7.53	6.14	9.60	584.75	0.34
S17	7.42	6.60	9.30	400.65	0.23
S18	7.46	5.90	10.20	452.20	0.26
S19	7.47	5.99	8.80	207.20	0.12

Fig. 3. N-J tree relationship among *Diamesa* species, based on a dataset of 283 COI sequences. The specimens from Tibetan Plateau were highlighted by red branches. Bootstrap support value (1000 replicates) above 70% were shown above the branches. Vertical dark lines indicated species groups defined on the basis of adult male [Lencioni et al., 2021].

Рис. 3. Дерево, построенное методом ближайшего соседа между видами *Diamesa* на основе 283 последовательностей COI. Красные ветви соответствуют образцам с Тибетского нагорья. Значения Бутстрэп-поддержек (1000 репликаций) выше 70% показано над ветвями. Вертикальными темными линиями обозначены группы видов, определенные на основе взрослых самцов [Lencioni et al., 2021].

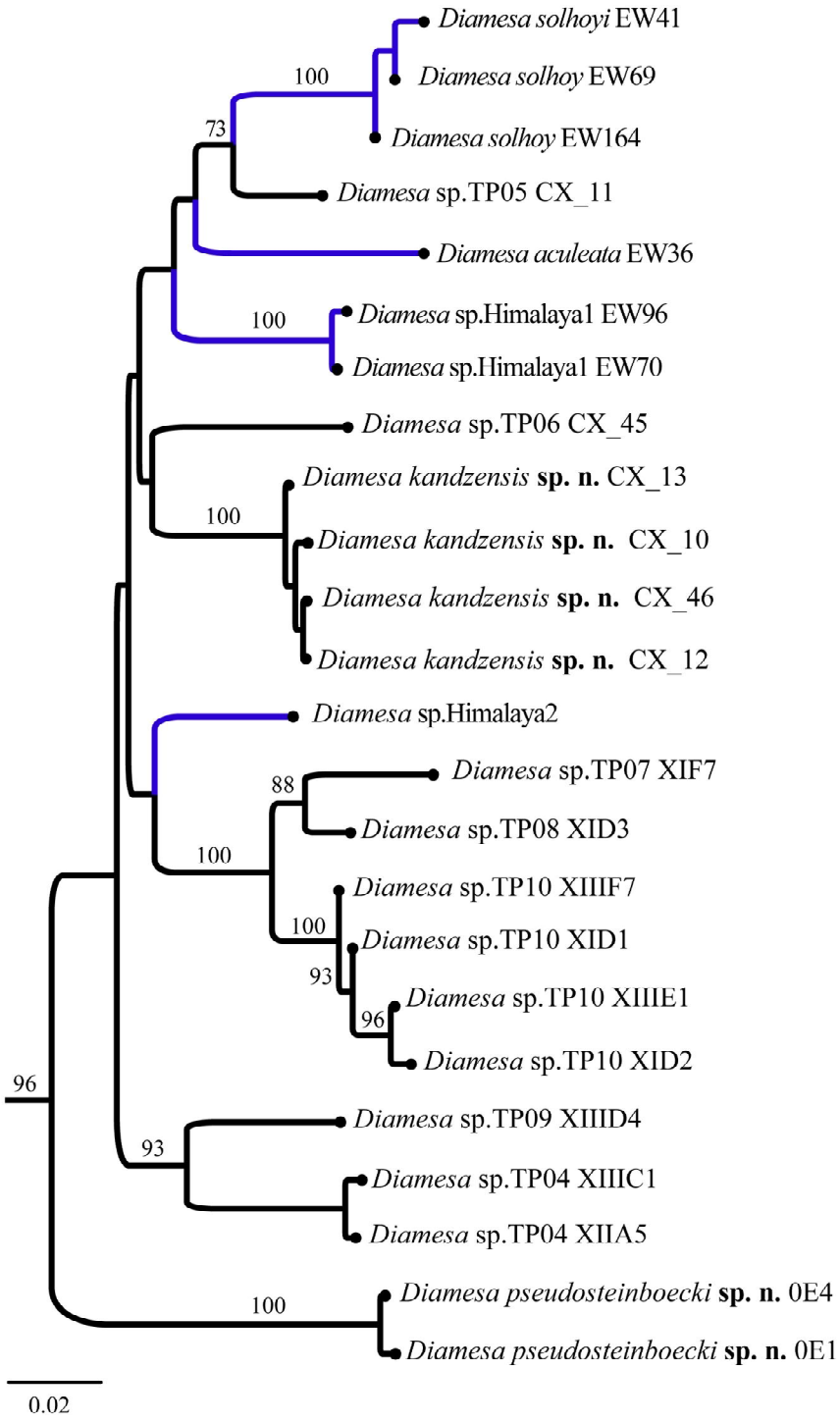

Fig. 4. N-J tree relationship among *Diamesa* species from Tibetan Plateau using 24 COII sequences. Seven sequences from Willassen [2005] were highlighted with blue branches. Bootstrap support value (1000 replicates) above 70% were shown above the branches.

Рис. 4. Дерево, построенное методом ближайшего соседа между видами *Diamesa* с Тибетского плато на основе 24 последовательностей COII. Красные ветви соответствуют образцам с Тибетского нагорья. Семь последовательностей из Willassen [2005] были выделены синими ветвями. Значения Бутстрэп-поддержек (1000 репликаций) выше 70% показано над ветвями.

Table 5. Genetic distance among putative molecular species
Таблица 5. Генетическая дистанция между предполагаемыми молекулярными видами

Species	n	Intra- and Interspecific K2P distance ()												
	Intra		Inter											
			1	2	3	4	5	6	7	8	9	10	11	12	13
1. *D. kandzensis*	4	1.14													
2. *D. kaszabi*	9	0.90	10.00												
3. *D. pseudosteinboecki*	2	0.33	13.48	12.72											
4. *D. qiangi*	4	0.49	10.09	3.61	12.35										
5. *D.* sp.TP01	1		9.87	9.34	9.89	9.26									
6. *D* .sp. TP02	1		9.81	8.57	12.00	8.87	5.28								
7. *D.* sp.TP03	1		10.08	10.40	13.36	11.30	8.77	8.35							
8. *D.* sp.TP04	2	0.79	12.18	10.39	12.85	11.10	9.55	8.88	10.85						
9. *D.* sp.TP05	1		10.68	8.45	11.59	8.40	7.51	7.55	9.11	9.82					
10. *D.* sp. TP06	2	0.32	11.24	9.16	12.17	10.20	7.98	8.72	10.24	10.79	8.33				
11. *D.* sp.TP07	1		6.66	7.54	12.26	7.39	6.81	6.43	7.42	8.89	6.81	8.59			
12. *D.* sp. TP08	2	0.79	7.56	9.06	12.55	8.53	6.56	7.46	9.30	9.79	7.92	9.49	4.46		
13. *D.* sp.TP09	1		9.41	10.86	12.14	10.65	8.06	8.73	10.11	9.01	9.15	9.61	6.57	5.41	
14. *D.* sp.TP10	5	1.04	8.94	9.08	12.61	8.66	8.06	7.99	9.62	9.92	7.87	10.4	4.84	3.6	5.39

Taxonomy Notes

Diamesa pseudosteinboecki Han et Tang, **sp.n.**

Fig. 5.

http://zoobank.org/NomenclaturalActs/ C87EEC04-7F98-4BC0-A6ED-F2C86A7327CE

Material. Holotype: male. Tibet, Ngari Prefecture, Rutog County, an unnamed small stream (S08) one kilometers upstream from the inlet of Spring Lake, 34.755029° N, 80.143951° E, alt. 5130 m, 13.viii.2021, leg. W. Han. Paratype, 4 males, 3 associated pupal exuviae, as previous.

Description. *Adult male* (n = 5, except when otherwise stated). Total length 2.68–3.20, 3.12 mm. Reduced wing 1.10–1.20 mm long, 0.25–0.26 μm wide. Total length/wing length 2.40–2.51 (n = 2) (Fig. 5D). Normal wing 1.75–1.82, 1.78 mm long, 0.48–0.54, 0.52 μm wide. Total length/wing length 1.45–1.80, 1.68 (Fig. 5E).

Coloration. Brown to dark brown (Fig. 5A).

Head. Eyes hairy, reniform. Temporal setae including 1–3 frontals, 4–5 orbitals, 3–5 verticals and 5–6 postorbitals. Clypeus with 2–3 setae. Antenna with 6–7 flagellomeres and reduced plume. Length of 1–7 flagellomeres (μm): 95–105, 102; 30–45, 43; 30–32, 31; 24–25, 25; 25–28, 26; 20–23, 21; 130–140, 138. AR 0.48–0.56, 0.54 (Fig. 5B). If 6 segments, each flagellomeres as follows (μm, n = 1): 75, 35, 30, 20, 20, 145. AR 0.69 (Fig. 5C). Palpomere length (μm): 20–28, 25; 40–48, 45; 75–80, 76; 60–63, 62; 70–85, 82. Palpomere 3 with sensilla capitata subapically, about 15 μm in diameter. Head width/palpal length 1.12–1.20 (n = 2). Antennal length/palpal length 1.25–1.30 (n = 2).

Thorax. Antepronotum with 6–10 ventrolateral setae. Dorsocentrals 6–8, prealars 5–6. Scutellum with 10–12 setae. AAII without setae.

Wing. Costal extension weak, 40–50 μm long. Anal lobe reduced. Squama with 1–2 setae. Venation normal. VR 0.87–0.90. R with 5–6 setae, R1 with 2–4 setae and R4+5 with 6–8 setae. RM/MCu 2.3–2.6, 2.5.

Legs. Spur of front tibia stout, 30–32 μm long. Both spurs of mid tibia 35 μm long. Spurs of hind tibia 35–40 μm and 58–60 μm long. Hind tibial comb with 16–18 setae. Length (μm) and proportions of leg segments are as in Table 6.

Hypopygium. Tergite IX with 12–16 setae, posterior edge nearly smooth, with oral-lateral corner rounded (Fig. 5F). Anal point, 55–65 μm long, slightly tapered towards the apex. Anal tergal bands Y-type; fused section 100–110 μm long. Transverse sternopodeme with triangular apex, 85–100 μm thick, 140–150 μm wide at the base. Gonocoxite 350–400 μm long, inner margin apparently without any lobe. Gonostylus 150–188 μm long, triangular, apical with a stout megaseta (10–12 μm long, 5–7 μm wide) and additional 1–2 subterminal teeth (Fig. 5G). HR 2.22–2.35.

Pupa (n = 3). Total length 3.56–3.85, 3.72 mm. Abdomen 2.70–2.85, 2.78mm.

Coloration (Fig. 5J, 5K). Golden-yellow to pale brown, seldom dark brown except for anal lobe.

Table 6. Lengths (мм) and proportions of leg segments of *Diamesa pseudosteinboecki* **sp. n.**, male (n = 5)
Таблица 6. Lengths (мм) и пропорции сегментов ног самца *Diamesa pseudosteinboecki* **sp. n.** (n = 5)

	fe	ti	ta1	ta2	ta3	ta4	ta5	LR	BV	SV
P1	1150–1275, 1213	1000–1125, 1063	580–650, 615	250–290, 268	140–160, 148	80	100–110, 105	0.56–0.60, 0.58	4.71–5.13, 4.82	3.64–3.79, 3.70
P2	1050–1250, 1163	875–950, 900	350–450, 405	160–190, 175	100–130, 115	70	90–110, 100	0.40–0.48, 0.45	5.16–5.67, 5.40	4.89–5.64, 5.12
P3	1150–1350, 1256	1000–1075, 1050	620–750, 695	330–390, 363	170–210, 185	70–85, 76	95–110, 103	0.62–0.68, 0.66	3.92–4.30, 4.14	3.15–3.55, 3.33

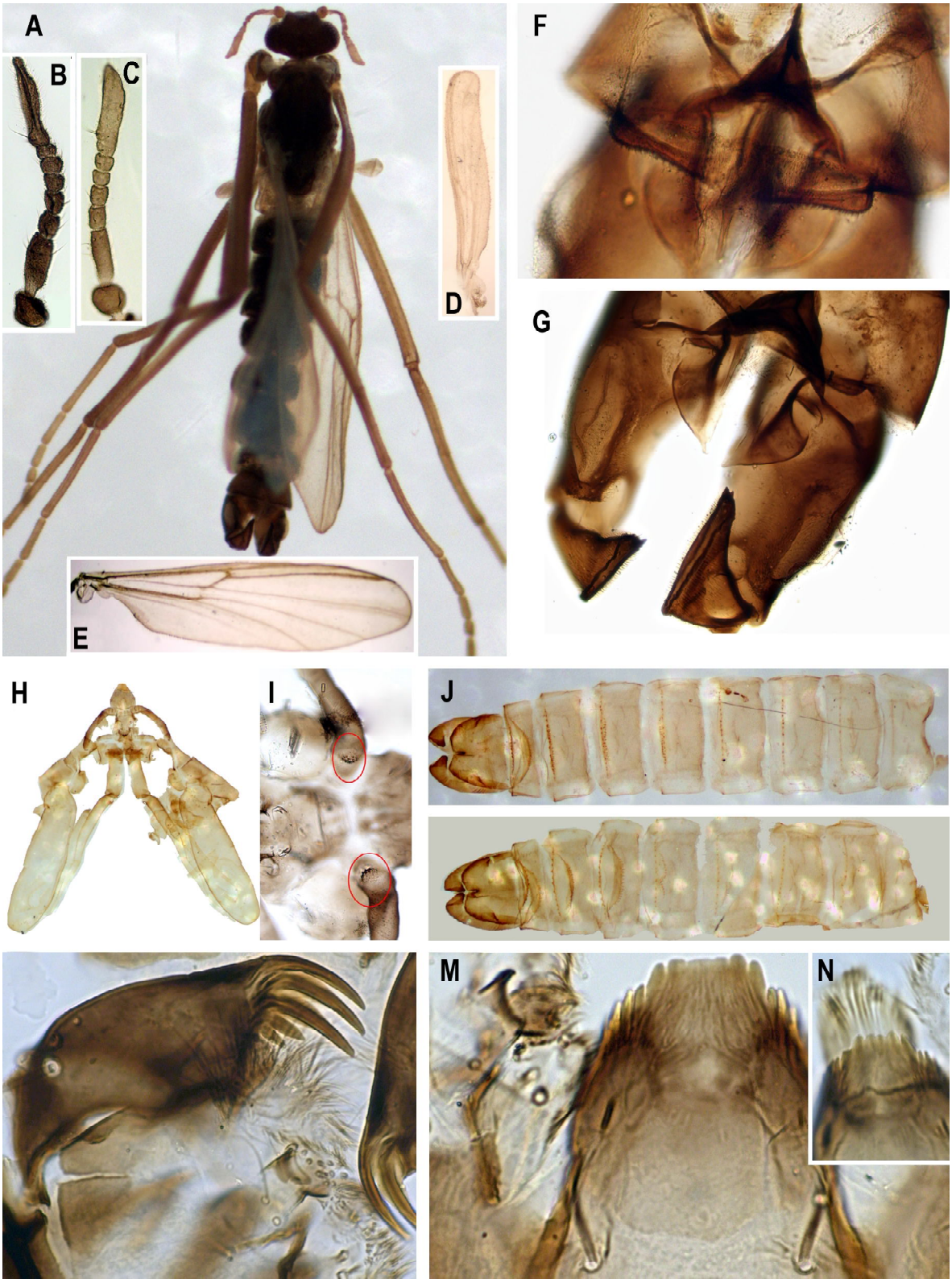

Fig. 5. Adult male of *D. pseudosteinboecki* **sp.n.** (A–G), pupa (H–K) and larva (L–N). A — adult male, dorsal view; B — 7-segment antenna; C — 6-segment antenna; D — reduced wing; E — normal wing; F — tergite IX, dorsal view; G — hypopygium, ventral view; H — cephalothorax; I — tubercle of pedicel sheath; J–K — pupal exuviae; L — mandible; M–N — mentum.

Рис. 5. Имаго самец *D. pseudosteinboecki* **sp.n.** (A–G), куколка (H–K) и личинка (L–N). A — имаго самец, вид сверху; Б — 7-сегментная антенна; C — 6-сегментная антенна; Д — редуцированное крыло; E — нормальное крыло; F — тергит IX, вид сверху; G — гипопигий, вид снизу; H — головогрудь; I — бугорок чехла базального членика антенны; J–K — экзувии куколки; L — мандибула; M–H — ментум.

Cephalothorax (Fig. 5H, 5I). Frontal seta 50–55 μm, two setae widely separated, the gap between them 150 μm. Tubercle of pedicel sheath well-developed, with dozens of small tubercles (Fig. 5I). Antepronotum and anterior part of thorax narrowed, with two precorneals, 50–60 μm long. Thoracic horn absent. Median suture of scutum with some wrinkles, Dc1/Dc2 grouped, and also Dc3/Dc4, all 25–30 μm long. Prealar tubercle broad, squashed.

Abdomen (Fig. 5J, 5K). Spinulation pattern as in *D. steinboecki*, e.g., all lateral setae very tiny, LS1and LS2 tightly grouped, 30–40 μm long. Median spinulation almost covering all the tergites of T III–VIII, dorsal thorn-like tubercle stout (12–15 μm high and 20–25 μm wide in base), ventral one slender and acute (20–25 μm high and 5–8 μm wide). Anal lobe rounded, 330–350 μm long, and 420–450 μm wide, with 2–3 short anal macrosetae, apically hooked,140–180, 150 μm long, 0.44–0.52 of anal lobe length. Male genital sac broad, clearly extending beyond anal lobe, apex with an inward curve towards the dorsal surface.

Larva (n = 1–2). Only partial head pieces remain.

Coloration. Head capsule light brown to brown, dark posterior occipital margin narrow.

Antenna. With 5 segments, each segments length (μm): 28–30, 10–12.5, 5–7, 2.5, 3.0. AR 0.92–1.20. Basal segment 2.6 times as long as wide. Blade and style not clear.

Labrum. SIII apparently multibranched. Premandible 60–65 μm long, with 6–7 teeth.

Mandible (Fig. 5L). 130–155 мм long, with 1 apical and 4 inner teeth, the first 2 inner teeth subequal to the apical teeth in the length, all those 3 teeth nearly paralleled, clustered, clearly longer than other two basal inner teeth. Seta interna with 24 branches.

Mentum (Fig. 5M, 5N). With 2 median teeth and 9 pairs of lateral teeth, first pair of laterals nearly fully fused with the worn median teeth, giving appearance of a truncate apex. Posterior extension of mentum well-developed, clearly beyond the location of seta submenti.

Diagnosis. The male and pupa cannot be clearly separated from *D. steinboecki* Goetghebuer. Generally, the larger AR (usu. > 0.5) and short anal point (< 70 мм) in the male of new species can be used to separate them. The pupa of new species with slightly longer and hooked anal macroseta, which differ from *D. steinboecki*, while in the larva, the different shape of mandible teeth is sufficient to separate them.

Диагноз. Имаго самец и куколка не могут быть четко отделены от *D. steinboecki* Goetghebuer. Как правило, для их разделения можно использовать более высокие значения AR (обычно > 0,5) и короткий анальный отросток (< 70 мкм) у самцов нового вида. Куколка нового вида с более длинными и крючковидно загнутыми анальными макрощетинками, что отличает их от *D. steinboecki*, тогда как для различия личинок можно использовать форму зубцоа мандибулы, которая у них разная.

Etymology. Refers to the similarity to *D. steinboecki* Goetghebuer in adult and immature stages.

Diamesa kandzensis Han et Tang, **sp.n.**

Fig. 6.

http://zoobank.org/NomenclaturalActs/92302281-85D1-4951-A9E2-74BE219969E1

Material. Holotype: a pharate male with pupal skin (CX-12). Sichuan Province, Garze Prefecture, Luding County, at Hongshitan of Hailuogou scenic spot (S02), 29.84002473° N 102.04106642° E, alt. 3073 m, 27.vi.2020, X. Wen. Paratype, 2 male pupae, 2 larvae, as previous.

Description. *Pharate male* (n = 2). Total length 4.40–5.90 mm. Wing length ca. 1.40–1.75 mm.

Coloration. Generally brown.

Head (Fig. 6A). Eyes bare, with weak dorsomedial extension. Temporal setae including 4 frontals, 4–6 orbitals, 8–10 verticals and 8–10 postorbitals. Clypeus with 8–12 setae. Antenna (Fig. 6B) with 13 flagellomeres, last flagellomeres 540 μm (n = 1). AR 0.96. Palpomere length (μm): 28–30; 35–40; 95–100; 100–105; 105–108. Palpomere 3 with sensilla capitata subapically, 15 μm in diameter. Head width/palpal length 1.32 (n = 1). Antennal length/palpal length 2.75 (n = 1).

Thorax. Antepronotals 3–4. Dorsocentrals 9–11, prealars 6–8. Scutellum with 14–16 setae with two rows. AAII without setae.

Wings shrink, all venation obscured. Squama with 26–28 setae.

Legs. Spur of front tibia 60–63 μm. Both spurs of mid tibia 40–45 μm long. Spurs of hind tibia 50–55 μm and 75–80 μm long. Hind tibial comb with 16–18 setae. Apex of Ta1 and Ta2 of all legs with paired pseudospurs. Apex of Ta_3 with pseudospurs only on the middle and hind leg. LR_1 0.64–0.67, LR_2 0.51–0.55, LR_3 0.70–0.81.

Hypopygium (Fig. 6C–F). Tergite IX with 14–16 setae. Anal point (Fig. 6E) 60–80 μm long, slightly tapered towards the apex. Gonocoxite 200–240 μm long, inner margin with a small basal lobe (superior volsella) in basal 1/3 (Fig. 6C), inferior volsella reduced or absent, only some weak trace (Fig. 6F). Gonostylus 150–170 μm long, apical with a slender megaseta, 10–12 μm long. HR 1.32–1.41.

Pupa (n = 2) Total length 4.43–5.88 mm. Abdomen 3.30–4.33 mm.

Coloration. Golden yellow.

Cephalothorax (Fig. 6G). Frontal seta 200–220 μm, two setae 100–140 μm separated. Tubercle of pedicel sheath absent. Antepronotals 3. Precorneals 2, 160–180 and 60–100 μm long, respectively. Thoracic horn 360–380 μm long, horn ratio 19–20. Median suture of scutum with granulations, only two Dcs present, the anterior longer, 120–140 μm long, the posterior 50–60 μm long. Prealar tubercle broad, triangular.

Abdomen (Fig. 6H). LS1and LS2 slightly separated, more subequal-distance in the middle section of abdomen (e.g., A. IV–VI). Median tiny spinules almost covering fully of T III–VIII, dorsal thorn-like tubercle squat (20–35 μm high and 30–40 μm wide in base), ventral teeth slender (40–65 μm high and 15–20 μm wide). Anal lobe 330–450 μm long, and 460–550 μm wide, with 3 anal macrosetae, apically hooked, 320–350. Male genital sac slightly extending beyond the distal margin of anal lobe, apex straight, not curved dorsally.

Larva (n = 1). Total length 4.6 mm. Head capsule 600 μm long and 420 μm wide.

Coloration. Head capsule dark brown, posterior occipital margin dark and relatively narrow.

Antenna (Fig. 6I) with 5 segments, each segment length (μm): 75, 12.5, 10, 2.5, 3.0. AR 2.14. Basal segment 4.30 times as long as wide. Blade 25 μm long, reaching to the apex of fourth segment.

Labrum. S_{III} bifid. Premandible (Fig. 6J) 87.5 μm long, with 7 teeth and several outer spines.

Mandible (Fig. 6K). 170 μm long, with 1 apical and 3 inner teeth, distally nearly paralleled and truncated. Seta interna with 24 branches.

Mentum (Fig. 6L). Apex truncated, with 12 flatten teeth, including one pair in the center median and additional 6–7 pairs teeth in the both lateral sides.

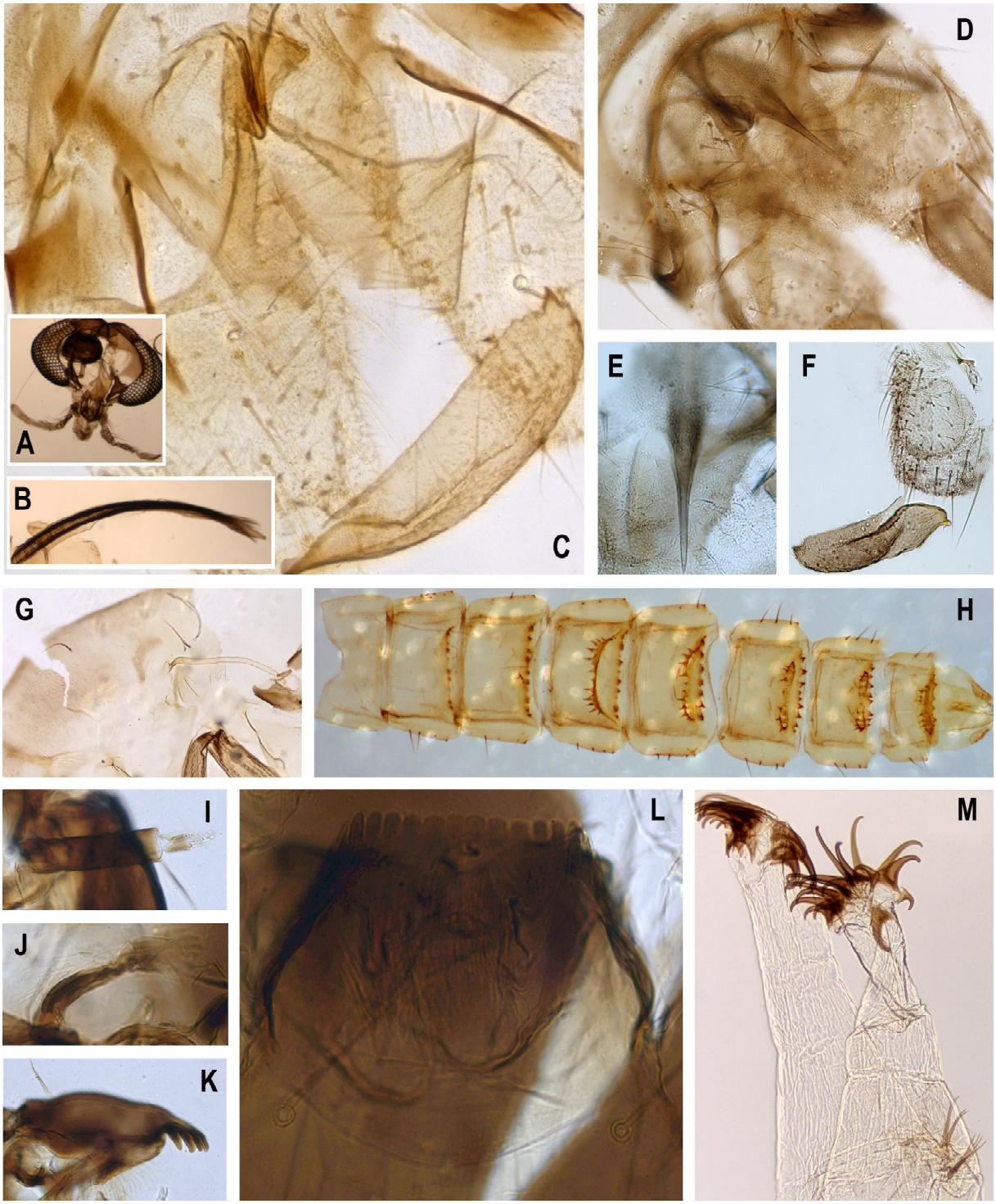

Fig. 6. Adult male of *Diamesa kandzensis* **sp.n.** (A–F), pupa (G–H) and larva (I–K). A — head; B — antenna; C — hypopygium, ventral view; D — hypopygium, dorsal view; E — anal point; F — inferior volsella and gonostylus; G — thorax (lateral view); H — pupal abdomen; I — antenna; J — premandible; K — mandible; L — mentum; M — posterior parapods.

Рис. 6. Имаго самец *Diamesa kandzensis* **sp.n.** (A–F), куколка (G–H) и личинка (I–K). A — голова; B — антенна; C — гипопигий, вид снизу; D — гипопигий, вид сверху; E — анальный отросток; F — нижний придаток гонококсита и гоностиль; G — грудь (вид сбоку); H — абдомен куколки; I — антенна; J — премандибула; K — mandible; L — ментум; M — задние подталкиватели.

Body. Anal segment (Fig. 6M) with 4 setae, 85–100 μm long. Posterior parapods 650 μm long and 270 μm wide in the base.

Diagnosis. The male hypopygium of new species resembles *D. pseudobertrami* Makarchenko, e.g., anal point long and slender, without obvious inferior volsella. The pupa resembles *D. bertrami* Edwards in the locations of abdomen lateral setae. However, new species can be separated from *D. pseudobertrami* by the lower AR in the male, and from *D. bertrami* pupa by the extensive spinulation in tergites III–VIII.

Диагноз. Гипопигий самца нового вида напоминает *D. pseudobertrami* Makarchenko, а именно, анальным отростком, который длинный и тонкий, нет явного нижнего придатка гонококсита. Куколка близка *D. bertrami* Edwards по расположению боковых щетинок брюшка. Новый вид можно отличить от *D. pseudobertrami* по более низкому значению AR у самца, а от куколки *D. bertrami* по обширной шагрени на тергитах III–VIII.

Etymology. From the type locality, Kandze, also spelling as Garze or Ganzi.

Diamesa kaszabi Serra-Tosio, 1983

Fig. 7.

Diamesa kaszabi, Serra-Tosio, 1983: 8.

Diamesa zelentzovi Makarchenko, 1989: 83.

Material. 2 adult males with associated pupal exuviae, Tibet, Ngari Prefecture, Geji County, Yare Township, Wamo Zangbo (S04), 31°29'57.6" N, 82°21'13.2" E, alt. 4816 m, 1.ix.2020, draft net, W. Han; 6 larvae, Tibet, Shikatse Prefecture, Ngamring County, Takkyel Tso (Daggyai Co) (S03), 29.807073° N, 85.745488° E, alt. 5151 m, 20.viii.2020; 4 larvae, Tibet, Ngari Prefecture, Geji County, Lalu Co (S14), 33.92084° N, 82.461553° E, alt. 4950 m, 19.viii.2021; 4 larvae, Tibet, Nagqu Prefecture, Shuanghu County, Purog Kangri Glacier NNR (S17), 33.950724° N 88.719499° E, alt. 5087 m, 29.viii.2021, leg. W. Han; 2 pupae with developing males. Tibet, Ngari Prefecture, Rutog County, an unnamed small stream (S12) one kilometer upstream from the inlet of Spring Lake, 34.755029° N, 80.143951° E, alt. 5368 m, 13.viii.2021, leg. W. Han.

Description. *Adult male* (n = 2). See Serra-Tosio, 1983. Two forms are found, total length of the larger form is ca. 7.0 mm, and the small form ca. 5.5 mm. The hypopygium (Fig. 7A–B) of two forms lack critical difference, some details of hypopygium see Fig. 7C (large form) and Fig. 7D–F (small form).

Pupa (n = 2). Total length 7.25 mm in large form, 5.38 mm in small form. Abdomen 5.50 mm for large form, 4.13 mm for small form.

Coloration. Golden yellowish brown or yellow (Fig. 7G–H).

Cephalothorax. Frontal seta 100–200 μm, two setae 120–130 μm separated. Antepronotals 3, 70–120 μm long, two median setae far away from the lateral one. Precorneals 3, 80–200 μm long, the middle longest and strongest, the anterior one weak. Thoracic horn 325–430 μm long, horn ratio 20–22. Median suture of scutum with dense granulations, only two Dcs present. Prealar tubercle broad, with granulations.

Abdomen. LS1 and LS2 grouped, separating from LS3 clearly. LS4 slender in thickness, ca. 2/3 length of LS3. Tergite I without any transverse band, but clear reticulations and wrinkles present. Spinules almost covering T III–VIII fully, dorsal thorn-like tubercle of large form triangular (90–100 μm high and 80–100 μm wide in base), stout in the small form (20–30 μm high and 30–35 μm wide in base), ventral teeth relatively slender (70–85 μm high and 50–60 μm wide in large form; 30–35 μm high and 20–30 μm wide in small form). Dark caudolateral corner tooth obvious, present in TII–TVIII. Anal lobe with anterior spinulation, 430–550 μm long, and 520–650 μm wide, with 3 anal macrosetae, apically hooked, 200–300. Male genital sac extending clearly beyond the distal margin of anal lobe.

Larva (n = 5). Median to large larva, total length 7.00–8.25, 7.35 mm. Head capsule 550–650, 594 μm long and 400–480, 445 μm wide.

Coloration. Head capsule dark brown, suffused with some paler and brown patches (Fig. 7J). Posterior occipital margin dark and thick.

Antenna (Fig. 7K). Each segment length (μm): 58–70, 63; 12.5–15, 13.8; 7.5; 3.0; 3.0. AR 1.72–2.33, 1.98. Basal segment 3.30–4.38, 3.90 times as long as wide. Blade 23–28, 26 μm long, reaching to the middle or apex of fourth segment. Accessory blade 15–20, 18 μm long, and style 8–10, 9 μm long.

Labrum. S_{III} simple. Premandible 80–90, 86 μm long, with 6–7 teeth and several outer spines.

Mandible (Fig. 7K). 140–170, 160 μm long, with 1 slender apical and 4 broad inner teeth, all normal packed. Seta interna with 14–18, 16 branches.

Mentum (Fig. 7L–M). With 1 single median tooth, 12–15, 13 μm wide, and 9–10 pairs of lateral teeth.

Body. Anal segment (Fig. 7O) with 4 normal anal setae, 250–300, 286 μm long, supraanal seta 60–80, 75 μm long. Posterior parapods 450–600, 580 μm long and 150–200, 180 μm wide in the base. Anal tubules (Fig. 7N) stout, 150–180, 160 μm long, 100–125, 120 μm wide in base, ca. 1/3 length of posterior parapods.

Remarks. Two forms of this species were collected from the same site, although the males have no critical difference, the abdominal thorn-like teeth in the pupae slightly differ, in the large form, the dorsal and ventral teeth are subequal in the size, while in the small form, the dorsal teeth are clearly stout than the ventral teeth. The median mental teeth are easy worn (Fig. 7J), which make it difficult to separate from *D. qiangi* described below.

Diamesa qiangi Wang et Makarchenko, 2019

Fig. 8.

Diamesa qiangi Wang et Makarchenko in Sun et al., 2019: 544.

Material. 1 adult male, Tibet, Nyingchi Prefecture, Dazivilla (S20), 29.54869° N, 94.47278° E, alt. 4282 m, leg. J. Liu; 3 larvae, Tibet, Ngari Prefecture, Purang County, an unnamed stream (S05), 30.821673° N, 81.542252° E, alt. 4625 m, 31.vii.2021, leg. Z.Y. Ni; 2 larvae, 1 pupa, Tibet, Ngari Prefecture, Gar County (S07), 31.168163° N, 80.925961° E, alt. 4752 m, 1.viii.2021, leg. Z.Y. Ni.

Description. *Adult male* (n = 1) (Fig. 8A). As described by Sun et al.[2019], except total length 4.85 mm, the last antennal flagellomere 570 μm.

Pupa (n = 1) (Fig. 8B). Total length 5.50 mm. Abdomen 3.88 mm.

Coloration. Golden yellow.

Cephalothorax. Frontal seta 150 μm, two setae 140 μm separated. Antepronotals 3, 80–200 μm long, two median setae far away from the lateral one. Precorneals 3, 80–200 μm long, the middle longest and strongest, the most anterior one weak. Thoracic horn 440 μm long, horn ratio 44. Median suture of scutum with dense granulations, only two Dcs present. Prealar tubercle broad, with granulations.

Abdomen (Fig. 8C). LS1 and LS2 grouped, separating from LS3 clearly. LS4 slender in thickness, less than 1/2 length of LS3. Tergite I without any transverse band, but with clear reticulations. Spinules covering T III–VIII fully, dorsal thorn-like tubercle larger (70–80 μm high and

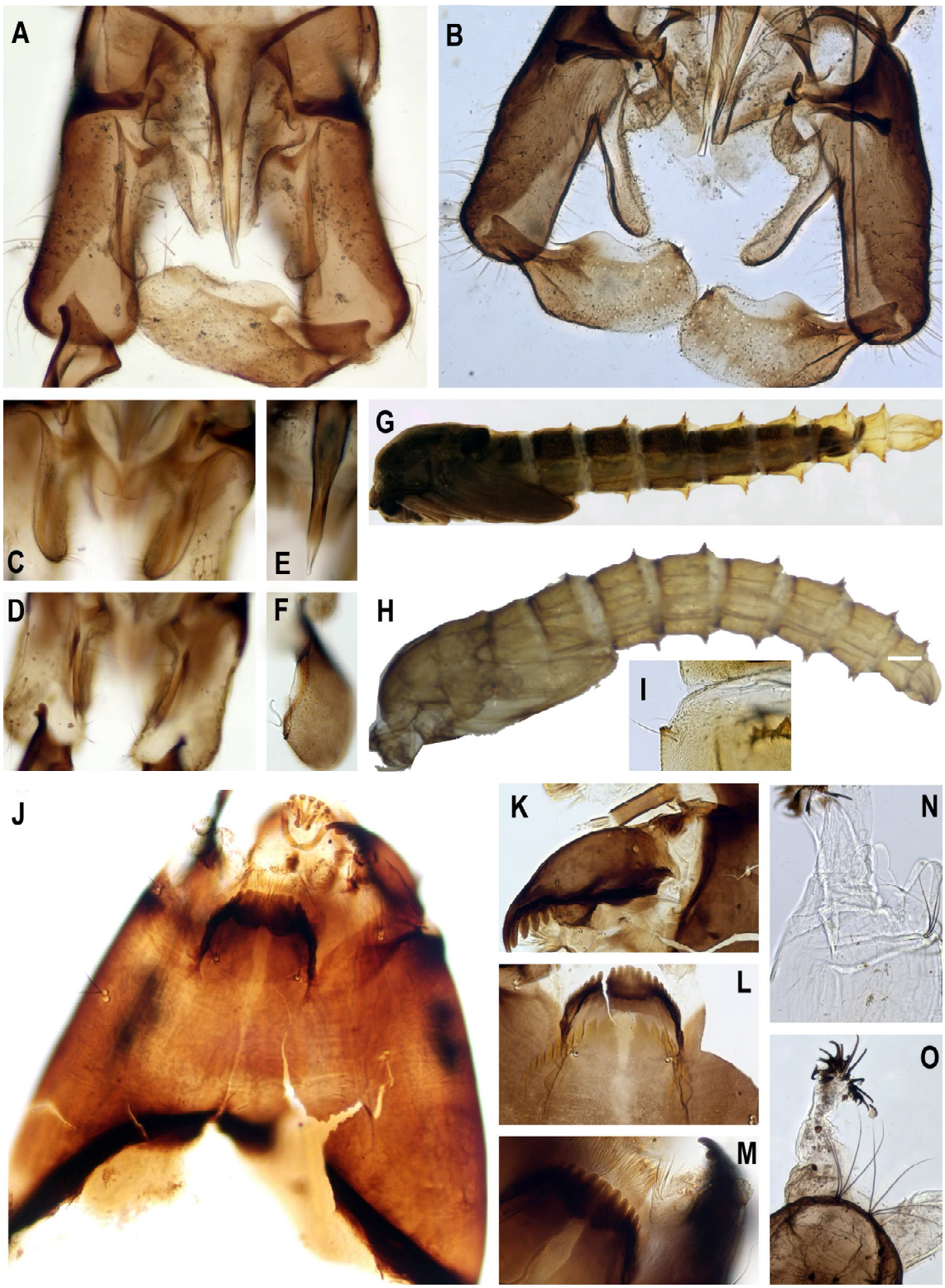

Fig. 7. Ault male of *Diamesa kaszabi* Serra-Tosio (A–F), pupa (G–I) and larva (J–O). A — hypopygium (large form); B — hypopygium (small form); C — inferior volsella (large form); D — inner margin of gonocoxite (small form); E — anal point (small form); F — gonostylus (small form). G–H — pupa, lateral view; I — corner teeth. J — head capsule; K — mandible; L–M — mentum; N — posterior parapods; O — anal setae.

Рис. 7. Имаго самец *Diamesa kaszabi* Serra-Tosio (A–F), куколка (G–I) и личинка (J–O). A — гипопигий (крупная форма); B — гипопигий (мелкая форма); C — нижний придаток гонококсита (крупная форма); D — внутренний край гонококсита (мелкая форма); E — анальный отросток (мелкая форма); F — гоностиль (мелкая форма). G–H — куколка, вид сбоку; I — угловые зубцы. J — головная капсула; K — мандибула; L–M — ментум; N — задник подталкиватели; O — анальные щетинки.

Fig. 8. Adult male of *Diamesa qiangi* Wang et Makarchenko (A), pupa (B–D) and larva (E–K). A — hypopygium; B — pharate male, dorsal view; C — pupal exuviae; D — corner teeth; E — antenna; F– mandible; G — premandible; H — labro-epipharyngeal region; I–J — mentum; K — anal setae.

Fig. 8. Имаго самец *Diamesa qiangi* Wang et Makarchenko (A), куколка (B–D) и личинка (E–K). A — гипопигий; B — выведенный самец, вид сверху; C — экзувий куколки; D — угловые зубцы; E — антенна; F– мандибула; G — премандибула; H — лаброфарингеальный район; I–J — ментум; K — анальные щетинки.

Table 7. Comparison between the named and defined code *Diamesa* species, larva (for abbreviations, see in the text)
Таблица 7. Сравнение названного и установленного кода вида *Diamesa*, личинка (сокращения см. в тексте)

Species	*kaszabi*	*qiangi*	*pseudosteinboecki*	*kandzensis*	sp. TP01	sp. TP02	sp. TP03	sp. TP04	sp. TP06	sp. TP08	sp. TP09	sp. TP10
TL	7.00–8.25	7.40–7.64	–	4.6	7.1	7.74	6.10–6.50	10.3–13.0	4.25	6.13–6.25	6.84	5.00–7.25
AR	1.72–2.33	1.90–2.08	0.92–1.20	2.14	2.13	1.86	1.32–1.50	2.56–3.00	1.82	2.00–2.15	2	2.00–2.36
A_1R	3.30–4.38	3.13–3.71	2.6	4.3	4.25	3.375	2.42–2.77	4.80–5.75	4	3.66–3.78	2.33	4.00–4.57
ROR	0.20–0.22	0.23–0.25	0.18	0.17	0.21	0.22	0.20–0.22	0.13–0.16	0.25	0.23–0.25	0.19	0.13–0.21
SPR	0.64–0.78	0.65–0.80	0.67	0.67	0.53	0.7	0.63–0.67	0.68–0.71	0.7	0.70–0.72	0.67	0.60–0.72
SIII	simple	simple/bifid	multibranched	bifid	bifid	simple	simple	simple	bifid	bifid	unknown	bifid
Md T shape	normal	normal	paralleled	paralleled	paralleled	normal	all reduced	reduced	normal	reduced	reduced	reduced
Si	14–18	18–20	24	24	42–45	20	16–18	16–28	20–22	24–35	28	22–28
Men. apex	normal	normal	smooth	truncated	truncated	normal	normal	normal	normal	truncated	smooth	truncated
Men. W.	125–140	130–160	60–65	125	140	150	95–115	170–180	95	132–140	145	120–140
Mid. tooth	single	bifid	bifid	notched	single, broad	bifid	single	single	notched	single	single	notched
SSm–SSm	100–120	100–115	50–55	105	58	115	80–95	110–130	80	100–110	100	100–105
Postmentum	280–320	270–310	175–200	255	350	350	235–250	500–510	240	300–325	340	280–315
AS	normal	normal	reduced	moderately	normal	normal	normal	reduced	normal	normal	normal	reduced
PPr	2.5–3.3	3.2–3.8	–	2.41	2.88–3.10	3.18	3.0–3.5	4.0–4.2	4.17	2.68–3.00	3.25	2.67–3.56

Table 8. Comparison between the described and defined code *Diamesa* species, pupa (for abbreviations, see in the text)
Таблица 8. Сравнение описанного и установленного кодового видов *Diamesa*, куколка (сокращения см. в тексте)

Species name	TL	Horn shape	Horn L	HR	Tergite median spinulation	Dorsal/ventral tubercle	Lateral seta distribution
*kaszabi*_large	7.25	tubular	430	22	fully covered	subequal	LS1&2 grouped
*kaszabi*_small	5.38	tubular	325	22	fully covered	squat/slender	LS1&2 grouped
qiangi	5.5	tubular	440	44	fully covered	subequal	LS1&2 grouped
pseudosteinboecki	3.56–3.85	tubular	absent	absent	fully covered	squat/slender	LS1&2 grouped
kandzensis	4.43-5.88	tubular	360–380	19-20	fully covered	subequal	intermediate
sp. TP03	6.10–6.50	tubular	350	20	fully covered	squat/slender	LS1&2 grouped
sp. TP05	6.25	tubular	450	32	fully covered	subequal	LS1&2 grouped
sp. TP07	6.25–6.85	spined conical	650-680	20–25	bare	squat/slender	subequal-distanced

60–70 μm wide in base), ventral teeth relatively slender (40–50 μm high and 30–40 μm wide). Dark caudolateral corner tooth clearly present in TII–TVIII (Fig. 8D). Anal lobe 460 μm long, and 540 μm wide, anterior 1/2 covering the spinulation, 3 anal macrosetae apically hooked, 260–280. Male genital sac clearly extending beyond the distal margin of anal lobe.

Larva (n = 3–4). Median to large larva, total length 7.40–7.64, 7.50 mm. Head capsule 630–650, 635 μm long and 440–450, 447 μm wide.

Coloration. Head capsule dark brown, color intensity fairly uniform in final instars. Posterior occipital margin dark and thick.

Antenna (Fig. 8E). Each segment length (μm): 58–65, 63; 12.5–15, 14; 5–10, 7.5; 2.5–3.0, 2.8; 3.0. AR 1.90–2.08, 2.00. Basal segment 3.13–3.71, 3.42 times as long as wide. Blade 23–25, 24 μm long, reaching to the basal of fourth segment. Accessory blade 15–18, 17 μm long, and style 8–10, 9 μm long.

Labrum (Fig. 8H). SIII simple or slightly forked apically. Premandible (Fig. 8G) 80–90, 88 μm long, with 7–8 teeth and several outer spines.

Mandible (Fig. 8F). 160–170, 166 μm long, with 1 apical and 4 inner teeth, all teeth normally located. Seta interna with 18–22, 20 branches.

Mentum (Fig. 8I). With 1 bifid median tooth, 10–12.5, 12 μm wide, and 11–12 pairs of lateral teeth. In some aberrant form, the first 3 pairs and median tooth all absent (Fig. 8J).

Body. Anal segment (Fig. 8K) with 4 normal anal setae, 260–300, 285 μm long, supraanal seta 60–80, 72 μm long. Posterior parapods 550–600, 570 μm long and 150–170, 160 μm wide in the base. Anal tubules stout, 100–120, 116 μm long, 70–75, 72 μm wide in base, ca. 1/3 length of posterior parapods.

Remarks. *D. qiangi* is closest to *D. kaszabi* with weak COI divergence (Table 5), however, differences in all stages are clear, in the former, the elongated gonostylus, the slender thoracic horn (horn ratio ca. 40) and bifid median mental teeth in the larva are distinct, while in the latter, the spherical gonostylus, the relatively thick thoracic horn (horn ratio ca. 20), and the single median tooth in the larva, separate them.

Diamesa coded taxa (TP01–10)

The coded ten taxa are summarized in Table 7 for larva and Table 8 for pupa. In general, those «species» can be separated from each other by using the listed key characters in the tables.

Discussion

In this study, four named *Diamesa* species and 10 putatively coded taxa were delimitated from the Tibetan Plateau based on both morphological taxonomy and barcoding techniques, which further verified the highly endemic biodiversity over Tibetan [Favre et al., 2015]. Nevertheless, further cryptic species are expected from the peri-glacial streams, elsewhere than where we had surveyed. Particular priorities to these glacier-fed streams should be given specifically in further studies as they are extremely sensitive and highly vulnerable to global warming. Considering the ongoing reduction of glaciers on the Tibetan Plateau, it is urgent to evaluate the extinction risk and redistribution of *Diamesa* and the potential ecological effect caused by the biodiversity loss.

The newly generated intraspecific distance (0.3 %–1 %) and interspecific (3.6 %–13.5 %) K2P genetic distance from our *Diamesa* database are comparable to the results of European Alpes [Lencioni et al., 2021b]. Though DNA barcoding has been widely utilized to discriminate and delimitate insects, it is risky to erect a species solely on the divergence between the limited genetic sequences [Wiemers, Fiedler, 2007; Renaud et al., 2012, Michailova et al., 2021]. In chironomids, previous studies had shown that COI barcodes failed to delimitate some allied species in the *D. cinerella* group and *D. zernyi* group [Montagna et al., 2016; Lencioni et al., 2021b]. In our study, ten coded «species» should not be treated as formal scientific species until further evidence, such as associated adult males and newly obtained nuclear genes.

The optimal temperature for European *Diamesa* was calculated as 6–7 °C [Castella et al., 2001], but other studies also suggested that *Diamesa* could live in unstable channels with warmer temperatures, where other chironomids are not abundant [Lods-Crozet et al, 2001]. The water temperature of most Tibetan streams in this study is relatively high because these sites are subjectively selected along the roads. Another considerable factor is the distance from the sampling site to the nearest glacier. As well-known, *Diamesa* is more abundant in some krenal streams and glacial reaches [Lencioni, Rossaro, 2005; Hamerlik, Jacobsen, 2012], few of our sampling sites are purposely targeted onto the head water of glaciers, which yielded limited available material from only 18 % of total sites. Interestingly, *Diamesa* were not detected in central Himalayas and southeast Tibetan Plateau in this study where the glacier shrinkage is pronounced [Zhang et al., 2021]. Are *Diamesa* populations really declining in this region? If so, is the decline related to the melting glaciers? However, these questions are absolutely out of the scope of this study because the influence of muti-strategy sampling efforts and random sites selection could not be eliminated in this study. More comprehensive evidence including from paleolimnology are necessary to answer these questions.

In conclusion, our study indicates that a great number of cryptic biodiversity over Tibetan Plateau has not been well explored as our case of *Diamesa*. Comprehensive investigations and researches are urgently needed to provide a scientific foundation for the protection of the ecosystem on the Tibetan Plateau.

Acknowledgements

This research was supported in part by the second Tibetan Plateau Scientific Expedition and Research Program (STEP, 2019QZKK0202). The authors are genuinely grateful to Evgeniy A. Makarchenko (Far East Branch of the Russian Academy of Sciences) for inspection on Central Asian specimens, and also to Peter S. Cranston (Australian National University) for his critical review

on the early draft. We also thank Hiromi Niitsuma for discussion of some *Diamesa* species in Japan.

References

Anderson A.M., Kranzfelder P., Bouchard Jr R.W., Ferrington Jr L.C. 2013. Survivorship and longevity of *Diamesa mendotae* Muttkowski (Diptera: Chironomidae) under snow // Journal of Entomological and Acarological Research. Vol.45. P.22–26.

Ashe P., O'Connor, J.P. 2009. A World Catalogue of Chironomidae (Diptera). Part 1. Buchonomyiinae, Chilenomyiinae, Podonominae, Aphroteniinae, Tanypodinae, Usambaromyiinae, Diamesinae, Prodiamesinae and Telmatogetoninae // Irish Biogeographical Society & National Museum of Ireland, Dublin, 445 p.

Castella E., Adalsteinsson H., Brittain J.E., Gislason G.M., Lehmann A., Lencioni V., Lods-Crozet B., Maiolini B., Milner A.M., Olafsson J.S., Saltveit S.J., Snook D.L. 2001. Macrobenthic invertebrate richness and composition along a latitudinal gradient of European glacier-fed streams // Freshwater Biology. Vol.46. P.1811–1831.

Chen F., Zhang J., Liu J., Cao X., Hou J., Zhu L, et al. 2020. Climate change, vegetation history, and landscape responses on the Tibetan Plateau during the Holocene: a comprehensive review // Quaternary Science Reviews. Vol.243. P.106444.

Curry C.J., Gibson J.F., Shokralla S., Hajibabaei M., Baird D.J. 2018. Identifying North American freshwater invertebrates using DNA barcodes: are existing COI sequence libraries fit for purpose? // Freshwater Science. Vol.37. P.178–189.

Edgar R.C. 2004. MUSCLE: multiple sequence alignment with high accuracy and high throughput // Nucleic Acids Research. Vol.32. P.1792–1797.

Ekrem T., Stur E., Hebert P.D. 2010. Females do count: Documenting Chironomidae (Diptera) species diversity using DNA barcoding // Organisms Diversity & Evolution. Vol.10. P.397–408.

Favre A., Päckert M., Pauls S.U., Jähnig S.C., Uhl D., Michalak I., Muellner Riehl A.N. 2015. The role of the uplift of the Qinghai Tibetan Plateau for the evolution of Tibetan biotas // Biological Reviews. Vol.90. P.236–253.

Flory E.A., Milner, A.M. 2000. Macroinvertebrate community succession in Wolf Point Creek, Glacier Bay National Park, Alaska // Freshwater Biology. Vol.44. P.465–480.

Folmer O., Black M., Hoeh W., Lutz R., Vrijenhoek R. 1994. DNA primers for amplification of mitochondrial cytochrome c oxidase subunit I from diverse metazoan invertebrates // Molecular Marine Biology and Biotechnology. Vol.3. P.294–299.

Hamerlik L., Jacobsen D. 2012. Chironomid (Diptera) distribution and diversity in Tibetan streams with different glacial influence // Insect Conservation and Diversity. Vol.5. P.319–326.

Han W., Tang H.Q. 2019. Phylogeny of marine *Ainuyusurika tuberculata* (Tokunaga) (Diptera: Chironomidae: Chironominae), with description of the immature stages // Zootaxa. Vol.4695. P.131–147

Han W., Wei J., Lin X., Tang H.Q. 2020. The Afro–Oriental Genus *Yaeprimus* Sasa et Suzuki (Diptera: Chironomidae: Chironomini): Phylogeny, New Species and Expanded Diagnoses // Diversity. Vol.12. P.31.

Hebert P.D., Gregory T.R. 2005. The promise of DNA barcoding for taxonomy // Systematic Biology. Vol.54. P.852–859.

Kumar S., Stecher G., Tamura K. 2016. MEGA7: molecular evolutionary genetics analysis version 7.0 for bigger datasets // Molecular Biology and Evolution. Vol.33. P.1870–1874.

Lencioni V. 2018. Glacial influence and stream macroinvertebrate biodiversity under climate change: Lessons from the Southern Alps // Science of the Total Environment. Vol.622. P.563–575.

Lencioni V., Rossaro B. 2005. Microdistribution of chironomids (Diptera: Chironomidae) in Alpine streams: an autoecological perspective // Hydrobiologia, 533, 61–76.

Lencioni V., Franceschini A., Paoli F., Debiasi D. 2021a. Structural and functional changes in the macroinvertebrate community in Alpine stream networks fed by shrinking glaciers // Fundamental and Applied Limnology. Vol.194. P.237–258.

Lencioni V., Rodriguez Prieto A., Allegrucci G. 2021b. Congruence between molecular and morphological systematics of Alpine non biting midges (Chironomidae, Diamesinae) // Zoologica Scripta. Vol.50. P.455–472.

Lin X.L., Chang T., Yan C.C., Wang B., Liu, W.B. 2021. Redescription of *Diamesa loeffleri* Reiss, 1968 (Diptera, Chironomidae) and new record from China // Annales Zoologici Fennici. Vol. 58. P.109–113.

Lin X.L., Stur E., Ekrem T. 2018. DNA barcodes and morphology reveal unrecognized species in Chironomidae (Diptera) // Insect Systematics & Evolution. Vol.49. P.329–398.

Lods-Crozet B., Castella E., Cambin D., Ilg C., Knispel S., Mayor-Sime´ant H. 2001. Macroinvertebrate community structure in relation to environmental variables in Swiss glacial stream // Freshwater Biology. Vol.46. P.1641–1661.

Makarchenko E.A. (Russian Academy of Sciences, Vladivostok, Russia), Tang, H.Q. (Jinan University, Guangzhou, Guangdong, China). 2022, Personal communication.

Makarchenko E.A., Semenchenko A.A., Palatov D.M. 2018. New data on taxonomy and systematics of the genus *Diamesa* Meigen (Diptera: Chironomidae: Diamesinae) from Tien Shan and Pamir Mountains, with description of two new species // Journal of Limnology. Vol.77. P.50–58.

Makarchenko, E.A., Semenchenko, A.A., Palatov, D.M. 2022. Taxonomy of *Diamesa steinboecki* group (Diptera: Chironomidae: Diamesinae), with description and DNA barcoding of new species. I. Subgroups *steinboecki* and l*ongipes* // Zootaxa. Vol.5125. P.483–512.

Michailova P., Lencioni V., Nenov M., Nikolov S. 2021. Can DNA barcoding be used to identify closely related Clunio Haliday, 1855 species (Diptera: Chironomidae, Orthocladiinae) // Zootaxa. Vol.4927. P.001–008.

Milner A.M., Robertson A.L., Monaghan K.A., Veal A.J., Flory E.A. 2008. Colonization and development of an Alaskan stream community over 28 years // Frontiers in Ecology and the Environment. Vol.6. P.413–419.

Montagna M., Mereghetti V., Lencioni V., Rossaro B. 2016. Integrated taxonomy and DNA barcoding of alpine midges (Diptera: Chironomidae) // PLoS One. Vol.11. P.e0149673.

National Snow and Ice Data Center (NSIDC), Global Land Ice Measurements from Space. 2019. RGI Qinghai Tibet Plateau glacier data (2015) // National Tibetan Plateau Data Center.

Puillandre N., Lambert A., Brouillet S., Achaz G.J.M.E. 2012. ABGD, Automatic Barcode Gap Discovery for primary species delimitation // Molecular Ecology. Vol.21. P.1864–1877.

Ratnasingham S. Hebert P.D.N. 2007. BOLD: The Barcode of Life Data System (http://www.barcodinglife.org) // Molecular Ecology Note. Vol.7. P.355–364.

Renaud A.K., Savage J., Adamowicz S.J. 2012. DNA barcoding of Northern Nearctic Muscidae (Diptera) reveals high correspondence between morphological and molecular species limits // BMC Ecology, 12, 24.

Rossaro B., Lencioni V. 2015. A key to larvae of *Diamesa* Meigen, 1835 (Diptera, Chironomidae), well known as adult males and pupae from Alps (Europe) // Journal of Entomological and Acarological Research. Vol.47. P.123–138.

Sæther O.A. 1980. Glossary of chironomid morphology terminology (Chironomidae, Diptera) // Entomologica scandinavica. Suppl.14. P.1–51.

Simon C., Frati F., Beckenbach A., Crespi B., Liu H., Flook P. 1994. Evolution, weighting, and phylogenetic utility of mitochondrial gene sequences and a compilation of conserved polymerase chain reaction primers // Annals of the entomological Society of America. Vol.87. P.651–701.

Stur E., Ekrem T. 2011. Exploring unknown life stages of Arctic Tanytarsini (Diptera: Chironomidae) with DNA barcoding // Zootaxa. Vol.2743. P.27–39.

Sun B., Lin X.L., Wang X.H., Makarchenko E.A. 2019b. New or little-known Diamesinae (Diptera: Chironomidae) from Oriental China // Zootaxa. Vol.4571. P.544–550.

Sun X.Y., Zhang R.J., Huang W., Sun A., Lin L.J., Xu H.G., Jiang D.C. 2019a. The response between glacier evolution and eco-geological environment on the Qinghai-Tibet Plateau // China Geology. Vol.2. P.1–7.

Wang X., Siegert F., Zhou A.G., Franke J. 2013. Glacier and glacial lake changes and their relationship in the context of climate change, Central Tibetan Plateau 1972–2010 // Global and Planetary Change. Vol.111. P.246–257.

Wiemers M., Fiedler K. 2007. Does the DNA barcoding gap exist? — a case study in blue butterflies (Lepidoptera: Lycaenidae) // Frontiers in Zoology. 4. 8.

Willassen E. 2005. New species of *Diamesa* (Diptera: Chironomidae) from Tibet: conspecific males and females associated with mitochondrial DNA // Zootaxa. Vol.1049. P.19–32.

Ye Q., Kang S., Chen F., Wang J. 2006. Monitoring glacier variations on Geladandong mountain, central Tibetan Plateau, from 1969 to 2002 using remote-sensing and GIS technologies // Journal of Glaciology. Vol.52. P.537–545.

Zhang G., Yao T., Xie H., Yang K., Zhu L., Shum C. K et al. 2020. Response of Tibetan Plateau lakes to climate change: Trends, patterns, and mechanisms // Earth-Science Reviews. Vol.208. P.103–269.

Zhang Y., Gao T., Kang S., Shangguan D., Luo X. 2021. Albedo reduction as an important driver for glacier melting in Tibetan Plateau and its surrounding areas // Earth-Science Reviews. Vol.220. P.103735.

Zhang Y., Ren H., Pan X. 2019. Integration dataset of Tibet Plateau boundary. National Tibetan Plateau Data Center, DOI: 10.11888/Geogra.tpdc.270099. CSTR: 18406.11. Geogra.tpdc.270099 (https://data.tpdc.ac.cn/en/data/61701a2b-31e5-41bf-b0a3-607c2a9bd3b3/, accessed date, 11 July 2022).

Поступила в редакцию 16.6.2022